The therapeutic potential of polymersomes loaded with ^{225}Ac evaluated in 2D and 3D in vitro glioma models

de Kruijff, R. M.; van der Meer, A. J.G.M.; Windmeijer, C. A.A.; Kouwenberg, J. J.M.; Morgenstern, A.; Bruchertseifer, F.; Sminia, P.; Denkova, A. G.

DOI
10.1016/j.ejpb.2018.02.008

Publication date
2018

Document Version
Final published version

Published in
European Journal of Pharmaceutics and Biopharmaceutics

European Journal of Pharmaceutics and Biopharmaceutics 127 (2018) 85–91

Contents lists available at ScienceDirect

European Journal of Pharmaceutics and Biopharmaceutics

journal homepage: www.elsevier.com/locate/ejpb

Research paper

The therapeutic potential of polymersomes loaded with ^{225}Ac evaluated in 2D and 3D in vitro glioma models

R.M. de Kruijff[a,*], A.J.G.M. van der Meer[a], C.A.A. Windmeijer[a], J.J.M. Kouwenberg[a], A. Morgenstern[b], F. Bruchertseifer[b], P. Sminia[c], A.G. Denkova[a]

[a] Radiation Science and Technology, Delft University of Technology, Mekelweg 15, 2629 JB Delft, The Netherlands
[b] European Commission, Joint Research Centre, Directorate for Nuclear Safety and Security, P.O. Box 2340, 76125 Karlsruhe, Germany
[c] VUmc Cancer Center Amsterdam, De Boelelaan 1118, 1081 HZ Amsterdam, The Netherlands

ABSTRACT

Alpha emitters have great potential in targeted tumour therapy, especially in destroying micrometastases, due to their high linear energy transfer (LET). To prevent toxicity caused by recoiled daughter atoms in healthy tissue, alpha emitters like ^{225}Ac can be encapsulated in polymeric nanocarriers (polymersomes), which are capable of retaining the daughter atoms to a large degree. In the translation to a (pre-)clinical setting, it is essential to evaluate their therapeutic potential. As multicellular tumour spheroids mimic a tumour microenvironment more closely than a two-dimensional cellular monolayer, this study has focussed on the interaction of the polymersomes with U87 human glioma spheroids. We have found that polymersomes distribute themselves throughout the spheroid after 4 days which, considering the long half-life of ^{225}Ac (9.9 d) (Vaidyanathan and Zalutsky, 1996), allows for irradiation of the entire spheroid. A decrease in spheroidal growth has been observed upon the addition of only 0.1 kBq ^{225}Ac, an effect which was more pronounced for the ^{225}Ac in polymersomes than when only coupled to DTPA. At higher activities (5 kBq), the spheroids have been found to be destroyed completely after two days. We have thus demonstrated that ^{225}Ac containing polymersomes effectively inhibit tumour spheroid growth, making them very promising candidates for future *in vivo* testing.

1. Introduction

Alpha-emitting radionuclides are ideal candidates to destroy tumour metastasis, especially those where it is of great importance to limit damage to surrounding healthy tissue. With their high linear energy transfer (LET) and short penetration ranges (~30 μm), just a few alpha tracks through the nucleus of a cell are sufficient to cause apoptosis. Because of their high energy-deposition, they cause mainly double-strand breaks in cellular DNA, which are difficult to repair. Non-repaired DNA double-strand breaks are lethal to the cell. Furthermore, alpha particles have a lower oxygen enhancement ratio (OER) [1], and are thus more capable of inducing damage in hypoxic cells or cancer stem cells. ^{225}Ac is a very promising radionuclide for targeted alpha therapy (TAT). With its relatively long half-life (9.9 d) [2] it has enough time to target also less-easily accessible tumours, and the 4 emitted alpha's in the decay chain ensure optimal damage once at the targeted site. However, upon the emission of an alpha particle, the daughter nuclide experiences a recoil energy. This recoil energy is several orders of magnitude larger than the energy of the chemical bond of the nuclide with a targeting antibody or peptide. The daughter nuclide will thus break free after the first decay, and will accumulate in other organs to damage healthy tissue in the subsequent decays [3]. Encapsulation in nano-carriers can be a solution to this problem [4,5], where (partial) retention of the daughter nuclides can be achieved. Polymersomes have shown to be very efficient in encapsulating ^{225}Ac and retaining it recoiling daughters [6,7]. These nanocarriers can be passively targeted to tumour tissue through the EPR effect, where the targeting efficiency can be further improved by attaching targeting moieties [8].

Pre-clinical in vitro studies are an integral part in development of potential new anti-cancer agents. While cell monolayer experiments are ideal for evaluation of effects at the cellular level, e.g. the localization in the cell where nanoparticles accumulate, they have limited value for predicting the therapeutic effect of anti-cancer compounds for actual tumours [9,10]. Three-dimensional tumour spheroids are a great intermediary between 2D cell cultures and *in vivo* models [10,11]. The physiological conditions of these spheroids far more closely resemble the microenvironment of actual tumours than their two-dimensional counterparts [12]. Depending on spheroid size, they develop chemical

* Corresponding author.
E-mail address: r.m.dekruijff@tudelft.nl (R.M. de Kruijff).

https://doi.org/10.1016/j.ejpb.2018.02.008
Received 11 October 2017; Received in revised form 5 February 2018; Accepted 7 February 2018
Available online 08 February 2018
0939-6411/

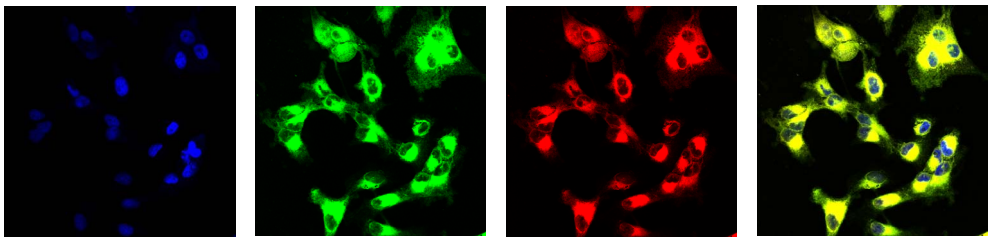

Fig. 1. Fluorescent microscopy images of a monolayer of U87 cancer cells, incubated with 100 nm FITC-labelled polymersomes at 4 h after addition of the polymersomes. The nuclei were stained with DAPI, and the lysosomes with Lysotracker Red.

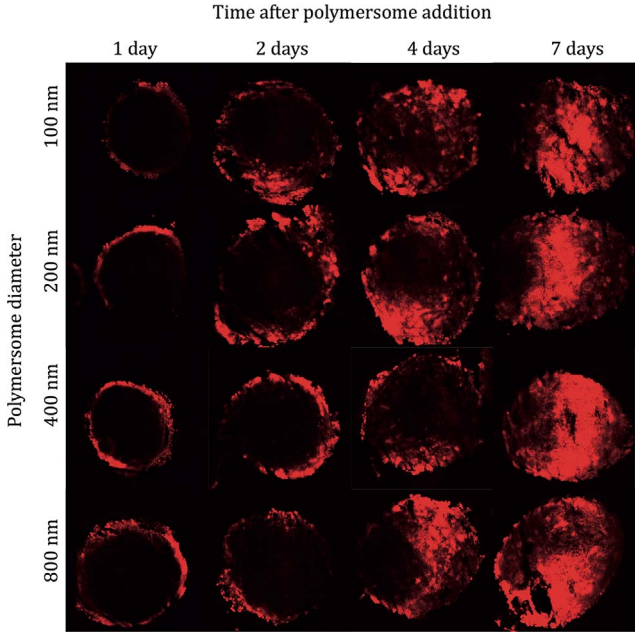

Fig. 2. Uptake of polymersome of different diameters, fluorescently labelled with PKH26 in U87 spheroids in time as measured by confocal microscopy, where the spheroid was sliced in 20 μm thick slices. *Note:* due to limitations of the confocal, only the fluorescence of the part of the spheroid that was in focus was imaged, but in fact for e.g. the 7d images the polymersomes were visible throughout the spheroid.

gradients [13], and even a centre containing hypoxic tumour cells [14]. The interaction between cells influences their size and shape, and which can directly influence cell functions [15]. The penetration and binding of (radio) pharmaceutics to cells is very different when working with 3D cell cultures, and more closely mimics the *in vivo* situation [13]. The presence of different mechanisms and the concomitant different phenotype makes spheroids a preferred model over adherent monolayer growing cells for studying effects of irradiation [16]. Recently, Gomez-Roman et al. has shown a differential effect in efficacy of a series of targeted drugs combined with irradiation between monolayer GBM cells and in a 3D model, the latter was found to be the most clinically representative and relevant for evaluation of new cancer therapies [17]. Similarly, a differential response to the combination treatment of irradiation with an AKT inhibitor between U251 glioma cells growing in monolayer or as multicellular spheroid was reported [18]. Hence, 3D spheroids are a valuable tool to determine their potential *in vivo*, and are increasingly used to evaluate new drugs [19].

In previous studies, we have encapsulated the alpha-emitting ^{225}Ac with high efficiency in polymersomes, which retained both the mother nuclide, as well as its alpha-emitting daughters very well [6]. In this study, the therapeutic potential of polymersomes loaded with ^{225}Ac has been evaluated in U87 spheroids. Furthermore, to better understand the observed effects we have investigated the localisation of the polymersomes in the glioma cells as well as the distribution of the nanocarriers within the spheroidal volume. We have compared the results with dose distributions determined by theoretical calculations.

2. Materials and methods

2.1. Chemicals

The poly(butadiene(1,2 addition)-b-ethylene oxide) block copolymer was obtained from Polymer Source (Quebec, Canada), with a Mn of 1900-b-900 g/mol, and a weight ratio (Mw/Mn) of 1.05. A dry ^{225}Ac sample was prepared at the Institute for Transuranium Elements, Karlsruhe, Germany [20]. The PD-10 columns were purchased from GE Healthcare, the 96-wells plates, 6-wells plates, the cell culture tubes and the 25 cm^2 cell culture flasks from Corning Inc, and the 30 mm cell culture petri dishes from Greiner Bio-One. The BioWhittaker Dulbecco's Modified Eagle's Medium (DMEM) and Hams F10 were purchased from Lonza (Verviers, Belgium). Sterile phosphate buffered saline (PBS) and 0.25% Trypsin- Ethylenediaminetetraacetic acid (Trypsin-EDTA) were obtained from Gibco (Paisley, UK), and Vectashield-DAPI from Vector Laboratories. All other chemicals were purchased from Sigma Aldrich (Zwijndrecht, The Netherlands).

2.2. Polymersome preparation and radionuclide labelling

Polymersomes were prepared by adding 2 mg block copolymers per 1 mL 4 mM PBS buffer solution at pH 7.4. The buffer solution contained 1 mM DTPA as hydrophilic chelate at pH 7.4 if it were to be used for radionuclide labeling. Polymersomes were extruded through polycarbonate filters with cut-off of 800, 400, 200 or 100 nm. The solution was stirred for a week, after which the polymersomes had formed. The polymersomes were loaded with ^{111}In or ^{225}Ac according to earlier published procedures [6,21]. In short, the free chelate was removed using a 30 cm Sephadex G 25 medium mesh column, after which 0.8 mL polymersome solution was added to a 0.2 mL 10 mM HEPES solution containing respectively a few MBq ^{111}In and 10 μL 2 mM tropolone solution or ^{225}Ac and 0.5 mg Ca-ionophore (A23187). After an incubation time of an hour, the unencapsulated radionuclides were removed using a PD10 purification column.

2.3. Fluorescent labelling of polymersomes

Polymersomes with diameters of 100, 200, 400 and 800 nm were labelled with PKH26 or FITC 'Isomer 1' fluorescent dye. 10 μl PKH26 (1 mM in ethanol diluted) or 2 μl FITC (10 mg/mL FITC in ethanol) was added to 1.0 mL polymersome solution. After 1 h incubation the free dye was removed by passing the solution through a PD10 column. Loading efficiency was determined by dissolving the loaded polymersomes at a 50:50 ratio in tetrahydrofuran (THF), and the sample was subsequently measured in a Fluorometer (Agilent). Retention was determined at 24 h after loading by centrifuging the polymersome sample at 2500 rmp for 30 min in an Amicon centrifuge tube with 50 KDa filter

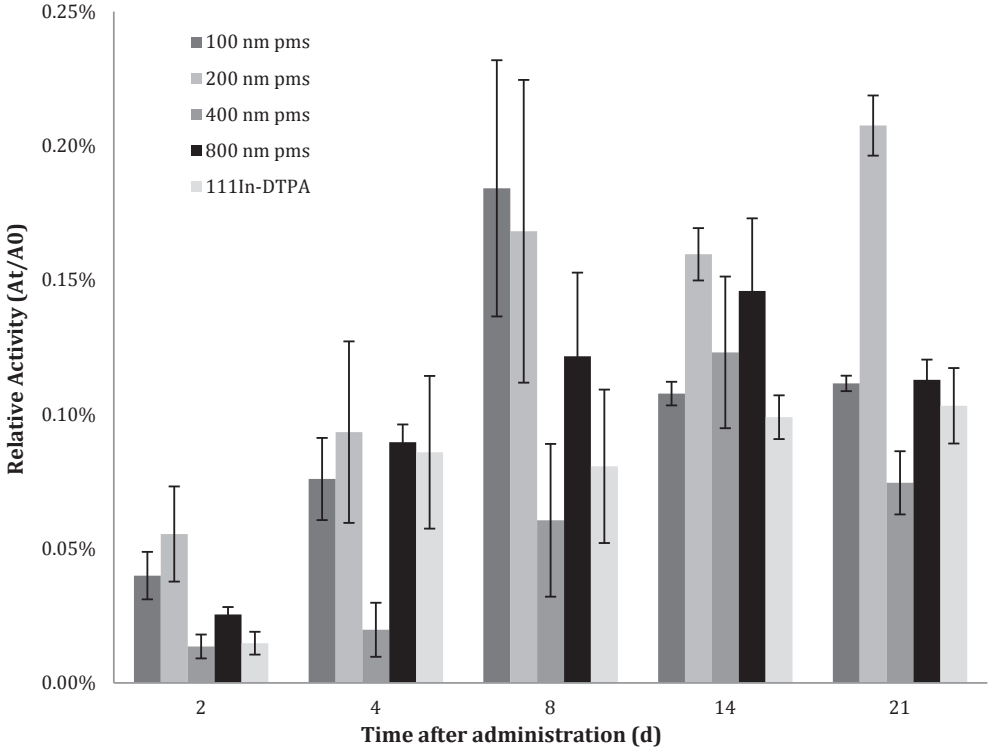

Fig. 3. Uptake of both polymersomes labelled with ^{111}In as a trace element, as well as ^{111}In-DTPA in spheroids.

(polymersomes are too large to pass the filter), and measuring the fluorescence signal of the liquid which had passed the filter.

2.4. Monolayer experiments

Polymersomes labeled with FITC were added to a U87 cells growing as monolayer. The U87 cell line was acquired from the ATCC. Cells were certified mycoplasma free by regular testing. For lysosome labeling experiments, 2 mL of 50 nM Lysotracker Red was added to the cells and incubated for 45 min. At different time intervals, the cell medium containing free polymersomes was removed and the cell was directly fixated with 3.7% PFA14. The PFA was allowed to incubate for 15 min at room temperature, after which the cells were rinsed with PBS. The cells were mounted with 4 µL Vectashield-DAPI16 and examined using a Leica LS5 confocal microscope.

2.5. Uptake of fluorescence labelled polymersomes in spheroids

For the formation of the spheroids, 5000 U87 glioblastoma cells were seeded in 96-well plates coated with 50 µL of 1.5% Agarose in DMEM and Pen/Strep. After one week, spheroids with diameter of 350–400 µm had formed. 50 µl of the labelled polymersomes was added in each well. After a specified duration (1 d, 2 d, 4 d, or 7 d), spheroids were harvested in a 2 mL Eppendorf vial. The spheroids were frozen using transparent tissue freezing medium (OCT) and glued on a pre-cooled cutting table. In the cryostat, 20 µm thick slices were cut at −25 °C, and in some cases Dapi vectashield was added to the slides [22]. Subsequently, the spheroids were imaged using Confocal Laser Scanning Microscopy with equal microscope settings.

2.6. Quantification of polymersome uptake in spheroids

A 50 µL polymersome solution labelled with 0.5 MBq of ^{111}In were added to the wells containing the spheroids in a similar fashion as the uptake experiments. After an incubation time between 1 and 21 days, the spheroid was removed and washed with 1 mL PBS. Subsequently, the ^{111}In activity in the spheroid was determined using an automatic gamma counter (Wallac 2480 Automatic Gamma counter Perkin Elmer Technologies) and corrected for decay.

2.7. Spheroid growth assay

The spheroids were formed according to the same procedure as used to determine the uptake of polymersomes. However, in these experiments 4 days after the cells were added to the wells either 50 µl of polymersome solution, containing different amounts of ^{225}Ac, or 50 µl PBS solution containing ^{225}Ac-DTPA was added. The growth of the spheroids was followed in time for up to 30 days by taking images through a binocular microscope with 50 × magnification (Olympus Tokyo CK, serial no. 206,904) with a normal camera (Olympus SZ-10, serial no. JEQ226246). The spheroid sizes in the images were analysed by ImageJ [23].

2.8. Dose calculations

The dose calculations on the spheroids were based on the results of the polymersome uptake, the pictures of the fluorescence labelled polymersomes and data on the energy loss of alpha particles in water obtained from NIST's ASTAR program [24]. The energy deposited by a single decay event was modelled as a rotationally symmetric 'energy' sphere in which the energy deposition density followed from the fluence and the Bragg peak of the respective alpha particle, both as function of distance from the distance of the energy sphere. The sum of the energy deposited in the energy sphere matched the total energy kinetic energy of the alpha particles produced in the ^{225}Ac decay chain (~28 MeV). This approach was chosen over an individual decay based Monte Carlo method for computational efficiency. For the polymersome-location matrix, uptake pictures were loaded into MATLAB for 200 nm polymersomes during day 1, 2, 4 and 7. The pictures were converted to greyscale and resized to form a near-perfect sphere. The 2D images were mapped onto a 3D matrix which would represent a perfect spheroid with internalized polymersomes. The matrices were

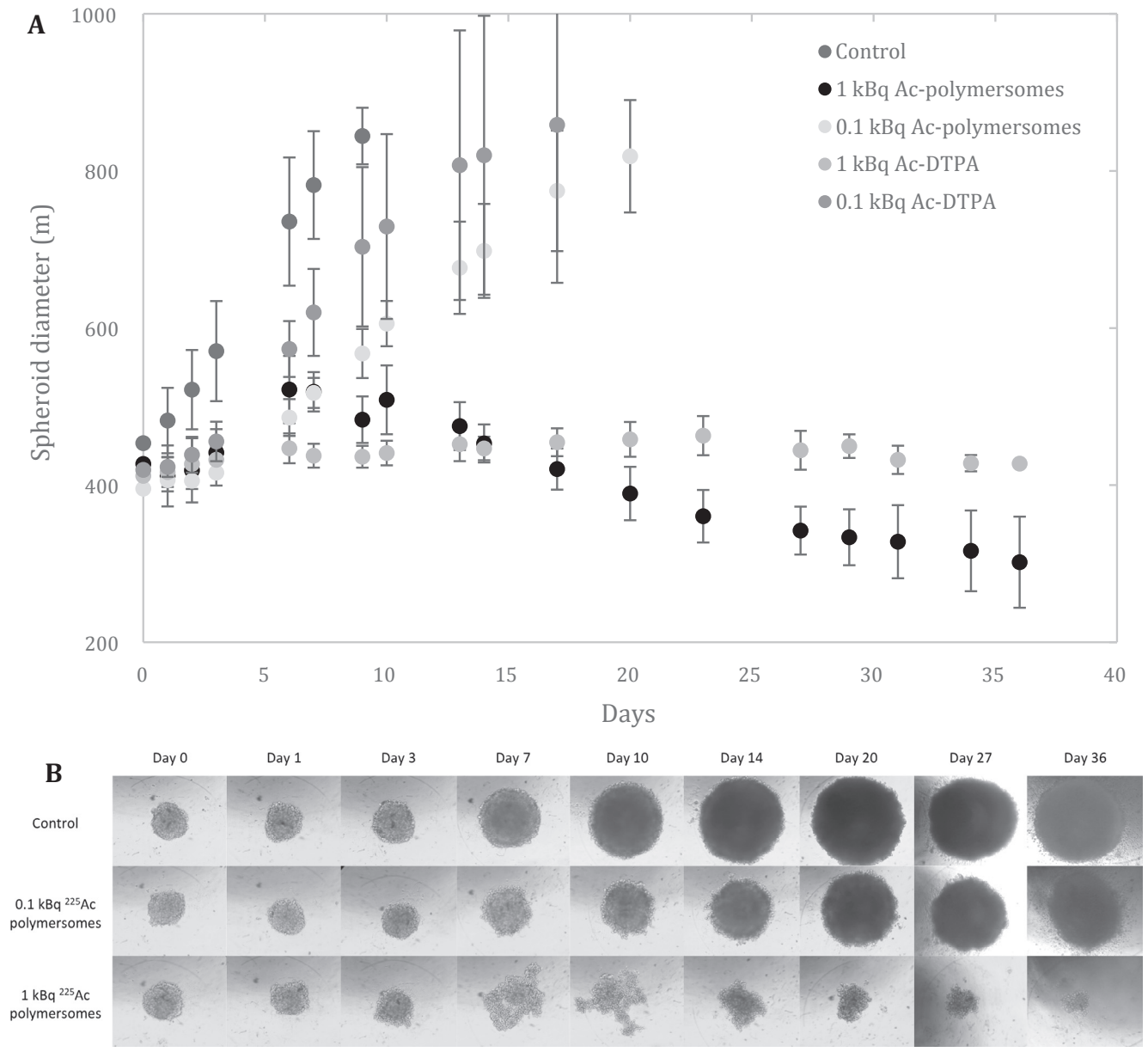

Fig. 4. (A) U87 tumour spheroid growth followed over more than a month, upon addition of either 1 kBq or 0.1 kBq of ^{225}Ac, encapsulated in 100 nm polymersomes, or attached to the chelator DTPA. Time-points where the spheroid growth has exceeded twice its initial diameter have been excluded as they were too large to follow their normal growth pattern. (B) Specific instances of U87 tumour spheroidal growth when challenged with ^{225}Ac-containing polymersomes as compared to 'normal' growth of the control group, followed for 36 days.

scaled for number of decayed particles during the time frame corresponding to the pictures used and the polymersome uptake during that day. The dose profile was subsequently calculated by the convolution of the four energy matrices with the pictures representing the diffusion of polymersomes into the spheroid (four in total). The sixteen resulting matrices were added up to obtain a total energy distribution.

3. Results

To get a better understanding of the role that polymersomes can play in alpha radionuclide therapy we have studied the localisation of polymersomes when internalised in cells as well as their distribution in 3D spheroids. Since alpha particles are short ranged, their distribution in the cell but also throughout the tumour is of great importance to ensure that sufficient cells are killed, in contrast to beta emitters which intra- and inter-cellular fate is of less importance. Furthermore, we have tried to determine any possible polymersome size limitations before moving to the in vitro evaluation of the therapeutic efficiency.

3.1. Polymersome preparation and radionuclide labelling

Polymersomes have been prepared at different average polymersome sizes (100, 200, 400 and 800 nm) as previously described [21]. The high stability of the fluorescent label, labelling efficiencies were 91 ± 14%, with practically no loss of fluorescent label (0.06 ± 0.02%) after 24 h, allowed for their use in subsequent in vitro studies. Radionuclide labelling efficiencies were consistently high, > 90% for ^{111}In and > 64% for ^{225}Ac, with < 5% and < 7% loss of radiolabel respectively [6,21].

3.2. Internalization and lysosome co-localisation in U87 cells

The internalisation and uptake mechanism of polymersomes have been determined in U87 glioblastoma cell monolayers. Uptake of the polymersomes has been found to be quite fast – polymersomes have already been detected in the cell cytoplasm after a few minutes. The uptake of polymersomes having a 100 nm diameter has been found not

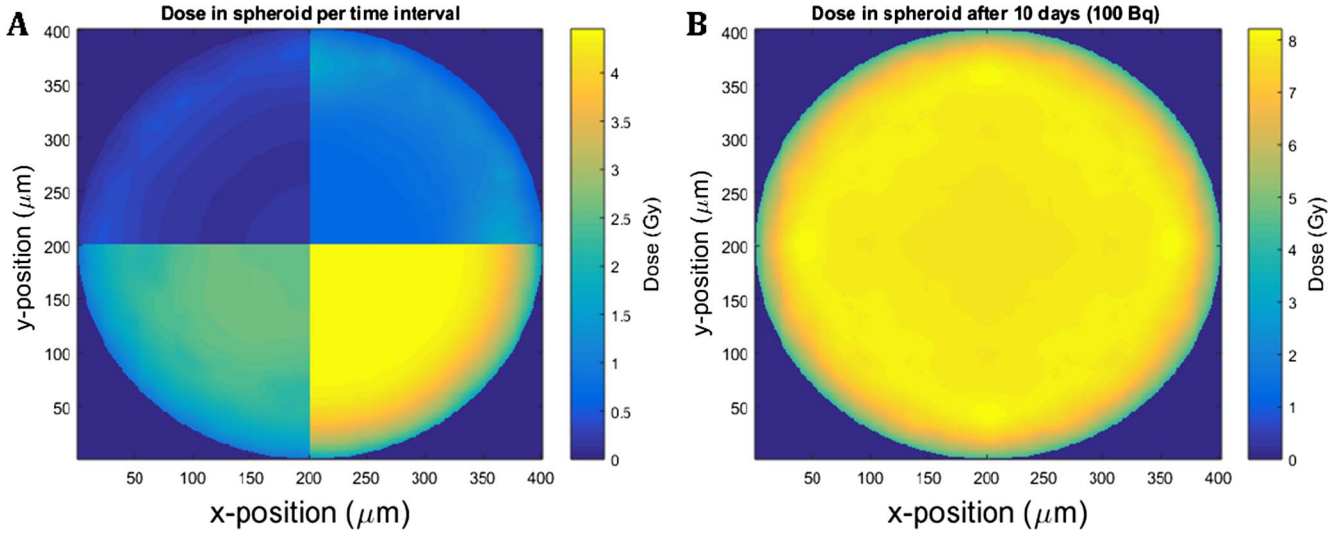

Fig. 5. (A) The dose in the spheroid at different times after addition of the polymersomes (day 1 – top left quarter, day 2 – top right quarter, day 4 – bottom left quarter and day 7 – bottom right quarter) and (B) cumulative dose distribution in the cross-section of a spheroid after 10 days, at an added activity of 0.1 kBq ^{225}Ac on day 0.

to change significantly after 3 h of incubation, reaching 2.5% ± 0.5% of the polymersomes having been taken up by the cells. As 3D models are more realistic tumour models, we have focused this study primarily on such models and thus not studied the uptake of all sizes in detail in 2D cell cultures. Rather, the 2D model has been used to show the localization of the polymersomes. In Fig. 1, the uptake and lysosome co-localisation of 100 nm FITC-labelled polymersomes is visualized by confocal microscopy. While the uptake has been visualised for all polymersome diameters (100 – –800 nm), no significant difference in uptake has been observed. After an incubation time of 4 h, polymersomes have been seen throughout the cytoplasm. No uptake in the cell nucleus has been observed due to the relatively large vesicle size, consistent with literature data [25]. To determine the uptake pathway, lysosomes have been labelled with Lysotracker Red.

Overlaying the images of the polymersomes and lysosomes shows a complete overlap of the fluorescent signal, indicating that the nanocarriers are, at least in part, taken up through endocytosis and end up in the lysosomes. Literature details that nanoparticles between 50 and 500 nm are internalized via clathrin-mediated endocytosis, and transported from early endosomes through late endosomes to lysosomes [30]. Although larger (> 750 nm) nanoparticles are generally taken up by phagocytic pathways instead of pinocytotic ones [31–33], we have not observed any difference between the small and large vesicles, which can be explained by the polydisperse nature of large polymersomes (those have passed only through a 800 nm extrusion filter, see also [6]), where the presence of the many small vesicles in the sample likely still causes the main uptake mechanism to be clathrin-mediated endocytosis.

3.3. Uptake of fluorescence labelled polymersomes in spheroids

The distribution of polymersomes in U87 tumour spheroids has been studied qualitatively in time, by imaging the fluorescent polymersome signal in 20 μm thick spheroid slices with confocal microscopy. In Fig. 2 the penetration of polymersomes through the spheroids has been visualized at different polymersome diameters. Although no quantitative conclusions can be drawn from this data, the images nicely illustrate the migration of polymersomes through the spheroids. Both the amount of fluorescence and the diffusion through the spheroid increased in time. After an incubation time of 1 day the polymersome concentration is significantly greater at the periphery of the spheroid as compared to the core. While uptake in a 2D cell culture is a relatively rapid process, diffusion throughout a 3D tumour is much slower, taking at least four days for the vesicles to distribute themselves completely (Fig. 2). The mechanism by which polymersomes diffuse through the spheroid is likely transcellular transport (endocytosis and subsequent exocytosis of the nanovesicles) [34,35].

After about 4 days the polymersomes have diffused nearly throughout the spheroid, and after 7 days the distribution was completely homogeneous. Although this might seem a relatively slow distribution of the polymersomes, the speed agrees quite well with literature values. A recent paper by Colley et al. has shown that polymersomes with 200 nm diameter take about five days to be distributed throughout the spheroid [36], which is similar to the distribution uptake rate determined in the present study. In fact, smaller particles (tens of nm in diameter) generally seem to spread faster through spheroids than larger vesicles (~100 nm) [37–39], although this naturally depends on, amongst others, shape, surface charge and solubility of the nanocarrier as well as cell type [40]. Studies with 100 nm PEGylated liposomes have also shown that at short incubation times (2–6 h), uptake is very limited and only visible in the outer rim of the spheroid [41,42], an effect which has also been reported *in vivo* [43]. This implies that while a longer time is needed for the diffusion of polymersomes through spheroids than for of smaller (< 100 nm) nanoparticles, the polymersomes do manage to diffuse throughout the entire spheroid. Multicellular spheroids larger than 500 μm diameter usually have hypoxic areas and a necrotic core [13]. The completely uniform distribution observed in our spheroids suggests that the polymersomes are also found in these areas. Combining excellent spheroid penetration with alpha radionuclide therapy ensures the destruction of both the proliferating outer cells as well as the hypoxic ones, which are the most challenging cells in tumour (radio)therapy [44,45]. However, despite the fact that spheroids are a much better representation of a real tumour than a cell monolayer, they still lack important tumour features such as an extracellular matrix and pressure gradients, which also play an important role in intratumoural nanoparticle distributions.

3.4. Quantification of polymersome uptake in spheroids

To quantify polymersome uptake in U87 spheroids, polymersomes labelled with ^{111}In have been added to the spheroids, and their uptake in the spheroids has been followed for 21 days (Fig. 3). ^{111}In was chosen as radiolabel since it has been shown to be retained in the vesicles to a very large degree (< 5% loss of radiolabel after 48 h) [21] and enables simple determination and quantification of the polymersomes. Furthermore, determination of cell survival through clonogenic essays in

2D models have allowed us to established that neither empty polymersomes nor polymersomes containing ^{111}In show any toxic effects nor influence cell proliferation. This is in good agreement with the findings of Amos et al., who have studied the toxicity of this particular type of polymersomes [46]. In the U87 spheroids, uptake has been found to stabilize around 0.10% of added activity after 8 days. No clear trend can be found between varying polymersome sizes, confirming the observations from the distribution experiments. Control experiments with ^{111}In-DTPA indicated similar spheroid uptake, although we have not been able to determine the distribution within the spheroid to see whether the ^{111}In-DTPA complex has resided mainly in the outer layers or has diffused to the centre as well. Uptake can be seen to steadily increase in time until about 8 d post-administration. Cell medium has not been replaced during this experiment to prevent dilution and removal of the polymersomes in the medium, resulting in a serum-deprived environment approximately 12 days after seeding (9 days after the addition of polymersomes). This coincides with the growth curve of the spheroids (data not shown), which stabilizes 12 days after seeding, which is also the point (> 8 d) at which polymersome uptake no longer increases. Cells enter the G0 phase upon serum deprivation, and eventually apoptosis will occur, though this takes longer in spheroids as compared to cell monolayers [26]. The rate of cellular uptake of nanoparticles is largely independent of the normal cell cycle [27], though during the G0 resting phase additional uptake will occur at a relatively low rate [28] and decrease further as they move towards apoptosis, thus explaining the stagnation in uptake from 14 days onwards (Fig. 3).

3.5. Spheroid growth experiments

The uptake profiles in spheroids indicate that polymersomes are ideally suited for enabling long-lived alpha-emitting radionuclides to accomplish uniform distribution throughout tumour metastasis, allowing for irradiation of all cells with little damage to surrounding healthy tissue. To this end, polymersomes labelled with the alpha-emitter ^{225}Ac have been tested in U87 spheroid cultures. In Fig. 4 the effect of either 1 kBq or 0.1 kBq of ^{225}Ac loaded in polymersomes on the spheroids is displayed. In all cases, growth of the spheroids has been inhibited by the addition of the radioactive vesicles, where as low as 0.1 kBq of ^{225}Ac already has a pronounced effect on spheroidal growth, and an increased activity of 1 kBq has led to a significant reduction in spheroid size. Challenging the spheroids with polymersomes containing 5 kBq ^{225}Ac resulted in the spheroid falling apart completely after two days (data not shown). Obtaining similar therapeutic efficacies with beta emitters would require much larger amounts of activity [29].

Control experiments where polymersomes without ^{225}Ac have been added to the spheroids showed that the vesicles themselves are not toxic. The addition of the exact same amount of ^{225}Ac to the spheroids, with the radionuclide attached to DTPA instead of encapsulated in the polymersomes, has resulted in reduced growth inhibition of the spheroids (Fig. 4). This implies that the nanocarriers are better capable of irradiating the spheroids than ^{225}Ac-DTPA as they inhibit spheroid growth to a larger degree at the same ^{225}Ac activity. This is mostly likely due to a better spheroid penetration combined with internalization in the cells, which allows them to be closer to the nuclei, as observed in the 2D studies, increasing the chance to hit the nuclear DNA. Using ^{111}In as analogue for the ^{225}Ac behaviour, we find that the relative uptake of ^{111}In-DTPA and ^{111}In in polymersomes is not significantly different (Fig. 3). The intra-spheroidal and intracellular distribution could explain the difference in tumour growth inhibition. Unfortunately, we have not been able to determine intercellular distribution for DTPA-complexes. The effect of vesicle distribution on spheroidal growth has also been shown by Zhu et al. [47]. They have compared ^{225}Ac encapsulated in non-targeted liposomes with ^{225}Ac-radiolabeled antibodies. The use of liposomes enhanced tumour killing efficiency due to the better interstitial distribution of the liposome, while the antibodies remained at the edge of the spheroid.

3.6. Dose calculations

The dose distribution has been estimated using experimental data of the polymersome distribution (Fig. 2) and uptake (Fig. 3) to get an idea of the dose necessary to induce the shrinkage of the tumours observed in the spheroid growth experiments. In Fig. 5 A the dose at different days after the addition of polymersome can be seen, where the final result of the sum of all convolutions is shown in Fig. 5B. This cumulative dose distribution shows that the minimum dose deposited in the spheroid is found in the rim (around 4 Gy), with a maximum deposited dose of 7.6 Gy after 10 days. The distribution visualized in Fig. 5 is equally representative of larger ^{225}Ac activities, the received dose increases linearly with added ^{225}Ac activity at equal polymersome concentration. The lower rim dose is due to the much lower polymersome concentration in the surrounding medium as compared to the spheroid, and the fact that the algorithm has interpreted some background values as being part of the spheroid by the algorithm, which cause low-intensity values that receive low dose in turn.

Comparing the irradiation damage induced by ^{225}Ac-containing polymersomes with other irradiation methods can help to estimate the killing potential of the alpha-emitter. However, nearly all studies have been performed with external radiation, making verification of the calculated radiation dose with literature tricky. While external irradiation of a spheroid is usually given in either one dose or in a number of smaller fractionated doses, the internally applied ^{225}Ac source in our experiments is continuously decaying and thus irradiates the spheroid over a long period of time. This can be seen as a continuous low dose rate irradiation or infinite fractionated irradiation exposures. Ho et al. found that there while there is a large difference in therapeutic effect between a single dose and the same dose in up to 8 fractions (1 log cell kill at 4–4.5 Gy and 7–8 Gy respectively), more than 8 fractions does not make much of a difference. The therapeutic effect we observed for an average alpha dose of 7.19 Gy is very similar to that found in their study for a fractionated 8 Gy X-ray dose over 15 days [48], showing the power of alpha radionuclide therapy at low activities. As can be seen in Fig. 4, in the first 15 days after 1 kBq of ^{225}Ac in polymersomes is added the spheroids stay more or less their initial size, after this time they start to shrink. This effect is similar to that found by Fedrigo et al. where they irradiated spheroid with up to 20 Gy [49]. Thus, our dosimetric model corresponds very well to literature data, and can accurately be used to predict spheroid growth inhibition at different ^{225}Ac-levels. Furthermore, it indicates that already at low radionuclide activity the ^{225}Ac polymersomes deliver a very high dose.

4. Conclusions

In the present study we have shown that vesicles with ^{225}Ac encapsulated in the aqueous cavity have enormous therapeutic potential, where spheroid growth inhibition is already observed at just 0.1 kBq of ^{225}Ac added. Spheroidal tumours start to shrink significantly at about 1 kBq of activity, and larger activities cause complete destruction of the spheroids after two days. A similar but smaller effect is observed for ‘free’ ^{225}Ac coupled to DTPA,. The better killing potential of the polymersomes is most likely due to their localisation around the cell nucleus as determined in 2D cell cultures of the same cell line. The fast uptake and the distribution of the polymersomes within the spheroid is also favourable for eventual therapeutic application. When comparing this to the very high amounts of beta-emitters required for a similar effect, the possibilities of applying this therapeutic radionuclide seem endless.

Acknowledgements

This study was funded by the SK foundation and the Zabawas foundation, and supported in part by the foundation STOPHersentumoren.nl, grant no. 2002657.

References

[1] G. Vaidyanathan, M.R. Zalutsky, Targeted therapy using alpha emitters, Phys. Med. Biol. 41 (1996) 1915–1931.
[2] S. Pommé, M. Marouli, G. Suliman, H. Dikmen, R. Van Ammel, V. Jobbágy, A. Dirican, H. Stroh, J. Paepen, F. Bruchertseifer, C. Apostolidis, A. Morgenstern, Measurement of the 225Ac half-life, Appl. Radiat. Isot. 70 (2012) 2608–2614.
[3] R.M. de Kruijff, H.T. Wolterbeek, A.G. Denkova, A critical review of alpha radionuclide therapy - how to deal with recoiling daughters? Pharmaceuticals 8 (2015) 321–336.
[4] S. Sofou, B.J. Kappel, J.S. Jaggi, M.R. McDevitt, D.A. Scheinberg, G. Sgouros, Enhanced retention of the alpha-particle-emitting daughters of Actinium-225 by liposome carriers, Bioconjug. Chem. 18 (2007) 2061–2067.
[5] J. Woodward, S.J. Kennel, A. Stuckey, D. Osborne, J. Wall, A.J. Rondinone, R.F. Standaert, S. Mirzadeh, LaPO4 nanoparticles doped with actinium-225 that partially sequester daughter radionuclides, Bioconjug. Chem. 22 (2011) 766–776.
[6] G. Wang, R.M. de Kruijff, A. Rol, L. Thijssen, E. Mendes, A. Morgenstern, F. Bruchertseifer, M.C.A. Stuart, H.T. Wolterbeek, A.G. Denkova, Retention studies of recoiling daughter nuclides of 225Ac in polymer vesicles, Appl. Radiat. Isot. 85 (2014) 45–53.
[7] R.M.de Kruijff, K. Drost, L. Thijssen, A. Morgenstern, F. Bruchertseifer, D. Lathouwers, H.T. Wolterbeek, A.G. Denkova, Improved 225Ac daughter retention in InPO4 containing polymersomes, Appl. Radiat. Isot. 1–24 (2017).
[8] D. Peer, J.M. Karp, S. Hong, O.C. Farokhzad, R. Margalit, R. Langer, Nanocarriers as an emerging platform for cancer therapy, Nat. Nanotechnol. 2 (2007) 751–760.
[9] J. Friedrich, R. Ebner, L. Kunz-Schughart, a Experimental anti-tumor therapy in 3-D: spheroids–old hat or new challenge? Int. J. Radiat. Biol. 83 (2007) 849–871.
[10] Y. Imamura, T. Mukohara, Y. Shimono, Y. Funakoshi, N. Chayahara, M. Toyoda, N. Kiyota, S. Takao, S. Kono, T. Nakatsura, H. Minami, Comparison of 2D- and 3D-culture models as drug-testing platforms in breast cancer, Oncol. Rep. 33 (2015) 1837–1843.
[11] L.-B. Weiswald, D. Bellet, V. Dangles-Marie, Spherical cancer models in tumor biology, NEO 17 (2014) 1–15.
[12] S. Skov Jensen, C. Aaberg-Jessen, I. Pind Jakobsen, S. Kjaer Hermansen, S. Kabell Nissen, B. Winther Kristensen, Three-Dimensional In Vitro Models in Glioma Research – Focus on Spheroids, in: D.A. Ghosh (Ed.), InTech, 2011.
[13] F. Hirschhaeuser, H. Menne, C. Dittfeld, J. West, W. Mueller-Klieser, L. Kunz-Schughart, a Multicellular tumor spheroids: an underestimated tool is catching up again, J. Biotechnol. 148 (2010) 3–15.
[14] P. Sminia, H. Acker, H.P. Eikesdal, P. Kaaijk, Oxygenation and response to irradiation of organotypic multicellular spheroids of human glioma, Anticancer Res. 23 (2003) 1461–1466.
[15] B.M. Baker, C.S. Chen, Deconstructing the third dimension – how 3D culture microenvironments alter cellular cues, J. Cell Sci. 125 (2012).
[16] I. Eke, N. Cordes, Radiobiology goes 3D: How ECM and cell morphology impact on cell survival after irradiation, Radiother. Oncol. 99 (2011) 271–278.
[17] N. Gomez-Roman, K. Stevenson, L. Gilmour, G. Hamilton, A.J. Chalmers, A novel 3D human glioblastoma cell culture system for modeling drug and radiation responses, Neuro. Oncol. 19 (2017) 229–241.
[18] R.S. Narayan, C.A. Fedrigo, E. Brands, R. Dik, L.J.A. Stalpers, B.G. Baumert, B.J. Slotman, B.A. Westerman, G.J. Peters, P. Sminia, The allosteric AKT inhibitor MK2206 shows a synergistic interaction with chemotherapy and radiotherapy in glioblastoma spheroid cultures, BMC Cancer 17 (2017) 204.
[19] G.Y. Lee, P.A. Kenny, E.H. Lee, M.J. Bissell, Three-dimensional culture models of normal and malignant breast epithelial cells, Nat. Methods 4 (2007) 359–365.
[20] C. Apostolidis, R. Molinet, G. Rasmussen, A. Morgenstern, Production of Ac-225 from Th-229 for targeted alpha therapy, Anal. Chem. 77 (2005) 6288–6291.
[21] G. Wang, R.M. de Kruijff, M.C.A. Stuart, E. Mendes, H.T. Wolterbeek, A.G. Denkova, Polymersomes as radionuclide carriers loaded via active ion transport through the hydrophobic bilayer, Soft Matter 9 (2013) 727–734.
[22] H.G. Augustin, Methods in Endothelial Cell Biology, Springer, Berlin Heidelberg, 2004.
[23] W. Rasband, ImageJ, U.S. Natl. Institutes Heal, 2016.
[24] M.J. Berger, J.S. Coursey, M.A. Zucker, J. Chang, ASTAR https://physics.nist.gov/PhysRefData/Star/Text/ASTAR.html.
[25] E. Oh, J.B. Delehanty, K.E. Sapsford, K. Susumu, R. Goswami, J.B. Blanco-Canosa, P.E. Dawson, J. Granek, M. Shoff, Q. Zhang, P.L. Goering, A. Huston, I.L. Medintz, Cellular uptake and fate of PEGylated gold nanoparticles is dependent on both cell-penetration peptides and particle size, ACS Nano 5 (2011) 6434–6448.
[26] S.-J. Lin, S.-H. Jee, W.-C. Hsiao, H.-S. Yu, T.-F. Tsai, J.-S. Chen, C.-J. Hsu, T.-H. Young, Enhanced cell survival of melanocyte spheroids in serum starvation condition, Biomaterials 27 (2006) 1462–1469.
[27] J.A. Kim, C. Åberg, A. Salvati, K.A. Dawson, Role of cell cycle on the cellular uptake and dilution of nanoparticles in a cell population, 2012.
[28] Liu Yan, W. Chen, P. Zhang, X. Jin, X. Liu, P. Li, F. Li, H. Zhang, G. Zou, Q. Li, Dynamically-enhanced retention of gold nanoclusters in HeLa cells following X-rays exposure: a cell cycle phase-dependent targeting approach, Radiother. Oncol. 119 (2016) 544–551.
[29] S.H. Cunningham, R.J. Mairs, T.E. Wheldon, P.C. Welsh, G. Vaidyanathan, M.R. Zalutsky, Toxicity to neuroblastoma cells and spheroids of benzylguanidine conjugated to radionuclides with short-range emissions, Br. J. Cancer 77 (1998) 2061–2068.
[30] L.M. Bareford, P.W. Swaan, Endocytic mechanisms for targeted drug delivery, Adv. Drug Deliv. Rev. 59 (2007) 748–758.
[31] Z. Mao, X. Zhou, C. Gao, Influence of structure and properties of colloidal biomaterials on cellular uptake and cell functions, Biomater. Sci 1 (2013).
[32] M. Zhu, G. Nie, H. Meng, T. Xia, A. Nel, Y. Zhao, Physicochemical properties determine nanomaterial cellular uptake, transport, and fate, Acc. Chem. Res. 622 (2013) 622–631.
[33] A. Parodi, C. Corbo, A. Cevenini, R. Molinaro, P. Roberto, L. Pandolfi, M. Agostini, F. Salvatore, E. Tasciotti, Enabling cytoplasmic delivery and organelle targeting by surface modification of nanocarriers, Nanomedicine 10 (2015) 1923–1940.
[34] H. Lu, R.H. Utama, U. Kitiyotsawat, K. Babiuch, Y. Jiang, M.H. Stenzel, Enhanced transcellular penetration and drug delivery by crosslinked polymeric micelles into pancreatic multicellular tumor spheroids, Biomater. Sci. 3 (2015) 1085–1095.
[35] A. Arranja, Development of Copolymer-based Nanocarriers for Imaging and Therapy, Université de Strasbourg, 2015.
[36] H.E. Colley, V. Hearnden, M. Avila-Olias, D. Cecchin, I. Canton, J. Madsen, S. MacNeil, N. Warren, K. Hu, J.A. McKeating, S.P. Armes, C. Murdoch, M.H. Thornhill, G. Battaglia, Polymersome-mediated delivery of combination anticancer therapy to head and neck cancer cells: 2D and 3D in vitro evaluation, Mol. Pharm. 11 (2014) 1176–1188.
[37] Y. Gao, M. Li, B. Chen, Z. Shen, P. Guo, M.L.-S. Guillaume Wientjes, J. Au, Predictive models of diffusive nanoparticle transport in 3-dimensional tumor cell spheroids, Am. Assoc Pharm. Sci. 15 (2013) 816–831.
[38] A.S. Mikhail, S. Eetezadi, S.N. Ekdawi, J. Stewart, C. Allen, Image-based analysis of the size- and time-dependent penetration of polymeric micelles in multicellular tumor spheroids and tumor xenografts, Int. J. Pharm. 464 (2014) 168–177.
[39] J. Wang, W. Mao, L.L. Lock, J. Tang, M. Sui, W. Sun, H. Cui, D. Xu, Y. Shen, The role of micelle size in tumor accumulation, penetration, and treatment, ACS Nano 9 (2015) 7195–7206.
[40] S. Barua, S. Mitragotri, Challenges associated with penetration of nanoparticles across cell and tissue barriers: a review of current status and future prospects, Nano Today 9 (2014) 223–243.
[41] K. Kostarelos, D. Emfietzoglou, A. Papakostas, W.-H. Yang, Å.M. Ballangrud, G. Sgouros, Engineering lipid vesicles of enhanced intratumoral transport capabilities: correlating liposome characteristics with penetration into human prostate tumor spheroids, J. Liposome Res. 15 (2005) 15–27.
[42] C. Zhu, M. Sempkowski, T. Holleran, T. Linz, T. Bertalan, A. Josefsson, F. Bruchertseifer, A. Morgenstern, S. Sofou, Alpha-particle radiotherapy: for large solid tumors diffusion trumps targeting, Biomaterials 130 (2017) 67–75.
[43] H. Cabral, Y. Matsumoto, K. Mizuno, Q. Chen, M. Murakami, M. Kimura, Y. Terada, M.R. Kano, K. Miyazono, M. Uesaka, N. Nishiyama, K. Kataoka, Accumulation of sub-100 nm polymeric micelles in poorly permeable tumours depends on size, Nat. Nanotechnol. 6 (2011) 815–823.
[44] M.R. Horsman, J. Overgaard, The impact of hypoxia and its modification of the outcome of radiotherapy, J. Radiat. Res. 57 (Suppl 1) (2016) i90–i98.
[45] B.-J. Hong, J. Kim, H. Jeong, S. Bok, Y.-E. Kim, G.-O. Ahn, Tumor hypoxia and reoxygenation: the yin and yang for radiotherapy, Radiat. Oncol. J. 34 (2016) 239–249.
[46] R.C. Amos, A. Nazemi, C.V. Bonduelle, E.R. Gillies, Soft Matter 8 (21) (2012) 5947.
[47] C. Zhu, T. Holleran, F. Bruchertseifer, A. Morgenstern, S. Sofou, Improved spheroid penetration of alpha-particle emitters by diffusing tunable liposomes for potential alpha-radiotherapy of solid tumors, J. Nucl. Med. 56 (2015) 1197–1197.
[48] J.-T. Ho, A. Sarkar, L.E. Kendall, T. Hoshino, laurence J. Marton, D.F. Deen, Effects of fractionated radiation therapy on human brain tumor multicellular spheroids, Int. J. Radiat. Oncol. 25 (1993) 251–258.
[49] C.A. Fedrigo, I. Grivicich, D.P. Schunemann, I.M. Chemale, D. dos Santos, T. Jacovas, P.S. Boschetti, G.P. Jotz, A. Braga Filho, A.B. da Rocha, Radioresistance of human glioma spheroids and expression of HSP70, p53 and EGFr, Radiat. Oncol. 6 (2011) 156.